

Percolation of the aligned dimers on a square lattice

V.A. Cherkasova¹, Yu.Yu. Tarasevich¹, N.I. Lebovka², and N.V. Vygornitskii²

¹ Astrakhan State University, 20a Tatishchev Str, Astrakhan, 414056, Russia

² Institute of Biocolloidal Chemistry named after F.D. Ovcharenko, NAS of Ukraine, 42, blvr. Vernadskogo, Kyiv, 03142, Ukraine

Received: date / Revised version: date

Abstract. Percolation and jamming phenomena are investigated for anisotropic sequential deposition of dimers (particles occupying two adjacent adsorption sites) on a square lattice. The influence of dimer alignment on the electrical conductivity was examined. The percolation threshold for deposition of dimers was lower than for deposition of monomers. Nevertheless, the problem belongs to the universality class of random percolation. The lowest percolation threshold ($p_c = 0.562$) was observed for isotropic orientation of dimers. It was higher ($p_c = 0.586$) in the case of dimers aligned strictly along one direction. The state of dimer orientation influenced the concentration dependence of electrical conductivity. The proposed model seems to be useful for description of the percolating properties of anisotropic conductors.

PACS. 64.60.Ak Renormalization-group, fractal, and percolation studies of phase transitions – 64.60.Cn Order-disorder transformations; statistical mechanics of model systems

1 Introduction

Physical properties of (partially) disordered systems are described in percolation approach [1,2,3,4,5,6,7]. Effect of concentration on physical properties is well understood. Nevertheless, alignment effect plays essential role for high aspect ratio objects, such as nanotubes and nanowires [8].

Percolating properties and behaviors of systems, composed of anisotropic nanoparticles, are extensively investigated during last years [9,10,11,12,13,14]. The problem of anisotropic percolation has been a subject of many investigations. It is of interest and of value to inquire how an orientation of nanoparticles influences the main physical properties of the systems. Effect of the nanotube alignment on conductivity is of specific interest. The anisotropy can be induced by various factors. For instance, alignment of the nanotubes may be induced by flow [8] or electric field [15,16].

The electrical properties of a ceramic composition were considered in [12]. A profound influence of the conducting phase structure on the electrical conductivity of the material was shown. The simulations indicated considerable dependence of the percolation cluster properties on anisotropy of its components.

The irreversible adsorption (deposition) of particles on solid surfaces is a subject of considerable practical importance. A well known example of an irreversible monolayer deposition process is the random sequential adsorption (RSA). RSA has attracted significant interest due to its importance in many physical, chemical, and biological processes. RSA is a natural model for irreversible and

sequential deposition of macromolecules at solid–liquid interfaces. Some examples of the wide range of applicability of this model include adhesion of colloidal particles, as well as adsorption of proteins to solid surfaces, with relaxation times much longer than the deposit formation time. This process is well described in the literature and has been investigated extensively in the last decades. The topic has been well covered in [17,18].

Investigation of the irreversible adsorption of polyatomic species (k -mers) has received considerable attention in the last years. The results of the study of random sequential adsorption and percolation of polyatomic species on different substrates were presented in [13,19,20,21,22,23,24,25,26,27,28]. Numerical studies of random sequential adsorption (the RSA model) of rectangular particles on a flat substrate are performed and dependencies of the saturation concentration and the percolation threshold on the model parameters are determined in [14].

The main goal of the present study is to investigate the influence of alignment on the percolation and jamming thresholds, as well as conductivity. In this paper, we provide accurate numerical data for the percolation and jamming thresholds of the (partially) ordered (aligned) dimers on a square lattice. We perform calculation of electrical conductivity as a function of dimers alignment. The proposed model can be useful for description of the percolation behaviour of anisotropic conductor networks.

The paper is organized as follows. In Section 2 the basis of the model of deposition of dimers on a square lattice is presented. The results, obtained using the finite size scaling theory, are also analysed and discussed in this Sec-

tion. The results, related to conductivity of the systems concerned, are presented in Section 3 pres. Finally, we discuss dependence of the percolation threshold on the model parameters of interest in Section 4.

2 Model and Simulations

Different kinds of boundary conditions were used in percolation simulations: open, periodic or toroidal, and cylindrical, i.e. open along one direction and periodic along another one. One uses usually the term crossing only to systems with open boundaries, and the terms spanning and wrapping for cylindrical boundary conditions [29]. In our study, the periodic boundary conditions are applied by gluing along the vertical and horizontal borders. We define a wrapping cluster as a cluster that winds around the system along the given direction, i.e. it provides a path with the length of 2π [29].

Mersenne Twister random number generator [30] was utilized for filling in the lattice with dimer at given concentration and orientation. It has a period of $2^{19937} - 1$.

The anisotropy of dimer orientation is described by the orientation order parameter s :

$$s = \frac{N_{|} - N_{-}}{N_{|} + N_{-}},$$

where $N_{|}$ and N_{-} are the numbers of dimers, oriented in vertical and horizontal direction, respectively [31].

Let us consider a periodic square lattice of linear size L , on which dimers are deposited at random, but with given orientation. Two of nearest neighbour sites along given direction are randomly selected; if both sites are vacant, the dimer adsorbs on such sites. Otherwise, the attempt is rejected. In any case, the procedure is iterated until $N = N_{|} + N_{-}$ dimers are adsorbed and the desired concentration is reached.

We perform our calculations of percolation thresholds using the Hoshen–Kopelman algorithm [32].

Fig. 1 demonstrates percolation in an anisotropic system of dimers (the dimers are oriented strictly along the vertical direction).

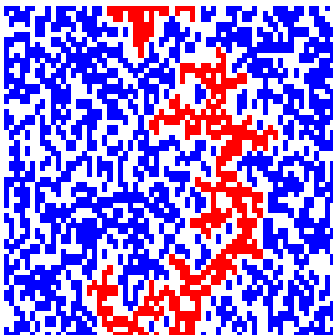


Fig. 1. Color online. Percolation on a square lattice of linear size $L = 64$ at $s = 1$ (wrapping cluster is indicated in red)

The final state, generated by irreversible adsorption, is a disordered state (known as jamming state), in which no more objects can be deposited due to the absence of any free space of appropriate size and shape [17]. If different orientations of the deposited objects are not equally probable, the definition of the jamming state is to be refined. Let us assume $N_{|} > N_{-}$. We define jamming for the fixed parameter s as a situation when there is no possibility of depositing any additional vertically oriented object. Nevertheless, there may be places for accepting horizontally oriented objects.

Fig. 2 shows jamming for different s at a lattice of linear size $L = 64$.

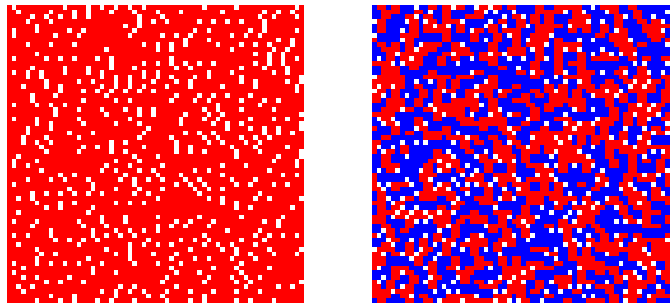


Fig. 2. Color online. Jamming at a lattice of linear size 64 at $s = -1$ (left) and $s = 0$ (right) (horizontally oriented dimers are shown in red, whereas the vertically oriented objects are shown in blue)

The percolation probability P vs. the site occupation probability p was obtained for the lattices of linear sizes $L = 64, 128, 256, 512, 1024$ and the number of runs 1000. The percolation probability P as a function of occupation p for a particular value of s is shown in Fig. 3. The percolation threshold p_c for a given lattice size L can be estimated from the condition $P(p) = 0.5$.

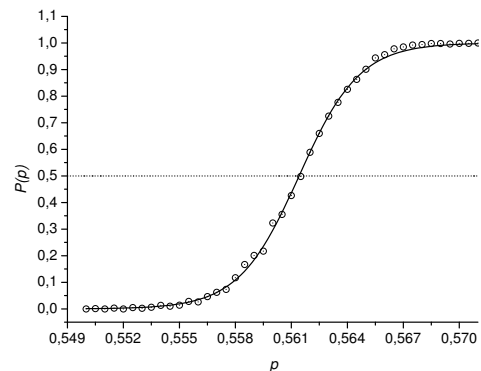


Fig. 3. Percolation probability P vs. occupation probability p for a lattice of linear size $L = 1024$ at $s = 0.4$, $p_c = 0.56141 \pm 0.00003$

The finite-size scaling analysis was carried out for getting the percolation threshold at $L \rightarrow \infty$. The percolation threshold $p_c(L)$ was calculated for five different values of

the linear lattice size. The percolation threshold $p_c(\infty)$ of an infinite lattice can be found by fitting the results for lattices of different sizes to the scaling relation (Fig. 4):

$$|p_c(L) - p_c(\infty)| \propto L^{-1/\nu}, \quad (1)$$

where the critical exponent ν has the value $4/3$ in three dimensions [6].

In particular, our simulations gave the percolation threshold $p_c = 0.5863$ for strictly oriented dimers ($s = 1$), and $p_c = 0.5617$ for dimers oriented in two directions with equal probability ($s = 0$). The last result agrees with the known results [22,28] (see Table. 1).

Table 1. Comparison of published and our results for dimers oriented in two directions with equal probability

	p_c	p_{jam}	p_c/p_{jam}
Our result	0.5617	0.90668	0.6195
Open boundary conditions, $L_{\max} = 2000$ [22]	0.562	0.906	$0,62 \pm 0.01$
Periodic boundary conditions, $L_{\max} = 112$, 5×10^4 runs [28]	0.562	0.907	0.6196

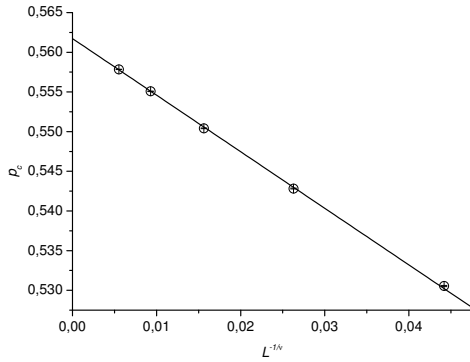


Fig. 4. Example of percolation threshold determination in the thermodynamical limit of ($L \rightarrow \infty$) using the scaling relation (1) ($s = 0$, $p_c = 0.56173 \pm 0.00003$)

Moreover, several quantities of interest [6] were calculated.

Average cluster size:

$$S = \frac{\sum_i n_i i^2}{\sum_i n_i i}, \quad (2)$$

where n_i is the average number of i clusters per lattice site.

The strength of the infinite network P_∞ , i.e. the probability of an arbitrary site belonging to the infinite network:

$$P_\infty(p) = \frac{N_\infty}{N}, \quad (3)$$

where N is the total number of sites.

The average cluster size S and strength of the infinite network P_∞ yield the scaling laws:

$$S(p) \propto |p - p_c|^{-\gamma}, \quad (4)$$

and

$$P_\infty(p) \propto (p - p_c)^\beta, \quad (5)$$

where γ and β the universal critical exponents. In $d = 2$ [35]:

$$\gamma = 2.3889, \quad (6)$$

and

$$\beta = 0.1389. \quad (7)$$

In our computations, the average cluster size (2) and the strength of the infinite network (3) demonstrate typical behavior near the percolation transition. The critical exponents $\gamma = 2.02 \pm 0.01$, at $p < p_c$, $\gamma = 2.37 \pm 0.05$, when $p > p_c$, and $\beta = 0.179 \pm 0.002$ for $s = 0$, extracted from the power laws (4) and (5), are close to the known values (6) and (7).

The fractal dimension of the incipient cluster [6], calculated as

$$d_f = d - \frac{\beta}{\nu}$$

, is close to the known values $d_f = 1.896$. For instance, $d_f = 1.8896$ for $s = 0$.

We found that parabolic law is a reasonable fit for p_c vs. s (Fig. 5).

The jamming threshold for $L \rightarrow \infty$ was found from scaling relation (1), where $\nu = 1.0 \pm 0.1$ is the critical exponent [22]. In particular, for strictly oriented dimers ($s = \pm 1$) (in fact, this case is quite equivalent to jamming in one dimension) $p_{jam} = 0.8646$, while exact value for jamming in one dimension is $p_{jam} = 1 - e^{-2} \approx 0.86466$ [17]. Fig. 5 demonstrates $p_{jam}(s)$.

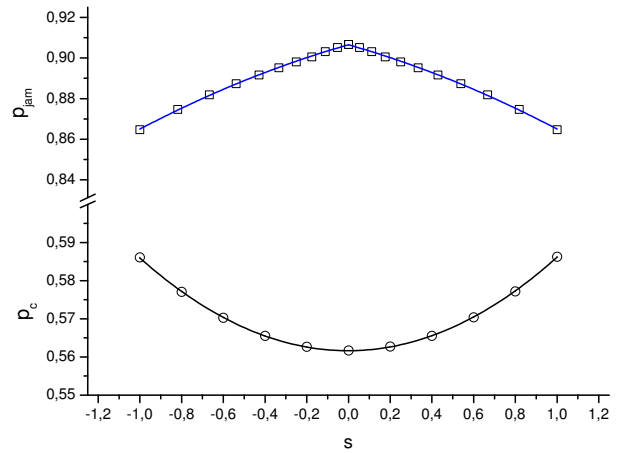


Fig. 5. Percolation threshold p_c vs. orientation order parameter s , $p_c(s) = 0.02442s^2 + 0.56165$, and jamming threshold vs. s , $p_{jam}(s) = -0.0124s^2 - 0.0291|s| + 0.9065$

3 Electrical conductivity

The highly efficient algorithm, proposed by Frank and Lobb [33] was utilized for finding conductivity of a square lattice, filled with the dimers.

The Frank and Lobb algorithm utilises the repeated application of a sequence of series, parallel and star-triangle ($Y-\Delta$) transformations to the bonds of the lattice. The final result of this sequence of transformations is reduction of any finite portion of the lattice to a single bond that has the same conductance as the entire lattice. We used four equivalent resistors (conductors) with $\sigma_f = 10^6$ and $\sigma_i = 1$ for occupied and empty sites [34], respectively, instead of each cell (see Fig. 6).

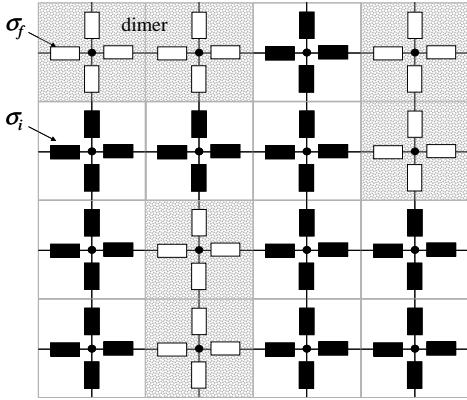


Fig. 6. Equivalent schema of a square lattice filled with dimers, where σ_f and σ_i are conductivity of the occupied side ($\sigma_f = 10^6$) and empty one ($\sigma_i = 1$), respectively

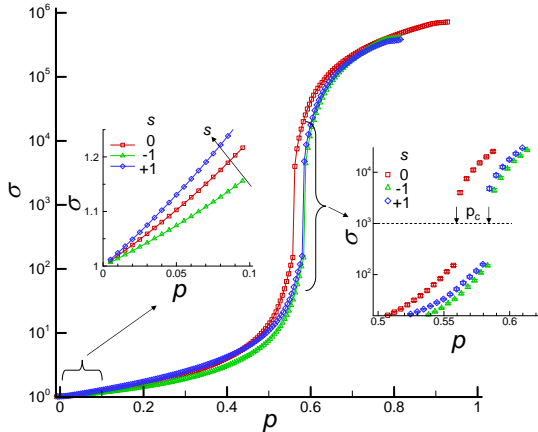


Fig. 7. Conductivity σ vs. occupation probability p for isotropic ($s = 0$) and strictly oriented dimers along the fixed direction ($s = \pm 1$). The lattice linear size is $L = 256$

Examples of conductivity σ as a function of occupation probability p at different values of parameter s are shown in Fig. 7. Behavior of the conductivity $\sigma(p)$ corresponds with direct estimations of the percolation threshold p_c .

There is a sharp transition of conductivity from σ_- to σ_+ near the percolation threshold (see right inset in Fig. 7). Moreover, σ increases on passing from isotropic ($s = 0$) to strictly ordered dimers ($s = \pm 1$).

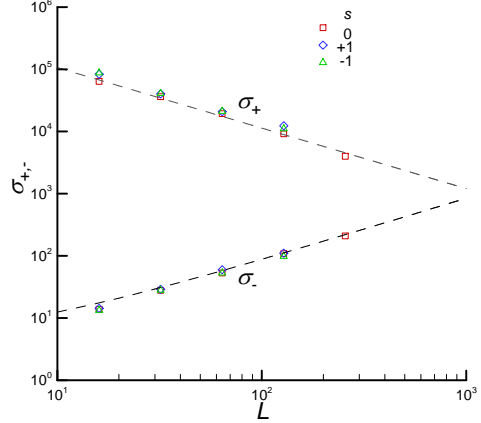


Fig. 8. Application of scaling to calculation of the ratio of conductivity exponent to the exponent of the correlation length for isotropic ($s = 0$) and strictly oriented ($s = \pm 1$) dimers. Dashed line corresponds to the slope 0.973, which is typical for percolation in two dimensions [36]

It is known that conductivity σ behaviour near the percolation threshold ($p - p_c \ll 1$) obeys the scaling relations [6]:

$$\sigma_- \propto (p_c - p)^{-s_c}, \quad p < p_c, \quad (8)$$

$$\sigma_+ \propto (p - p_c)^{t_c}, \quad p > p_c, \quad (9)$$

where t_c, s_c are the conductivity exponents.

A detailed study of the finite size effects is presented in order to discuss the universality class of the phase transition which the system undergoes. The main aim of the paper is to determine the dependence

For purposes of checking the universality class and calculating the values of t_c, s_c , the relations (8) and (9) can be written in the following form

$$\sigma_- \propto L^{s_c/\nu}, \quad p < p_c, \quad (10)$$

$$\sigma_+ \propto L^{-t_c/\nu}, \quad p > p_c, \quad (11)$$

where L is the linear lattice size [36].

Fig. 8 shows results of the finite-size analyzes of σ_- and σ_+ . Ratios of the conductivity exponents to the correlation length exponent t_c/ν and s_c/ν are independent of s and close to 0.973 ± 0.05 , which is a typical value for the percolation in $d = 2$ [36]. Hence, our model belongs to the class of random percolation in two dimensions. This statement agrees with the conclusion drawn from analysis of the exponents ν, γ, β .

Near the percolation point, behaviour of the conductivity depends essentially on s . At given p , the conductivity can fall down near the percolation threshold ($p \rightarrow p_c$) if alignment of dimers ($|s|$ increases). Thus, alignment induces decrease of the conductivity at given conditions.

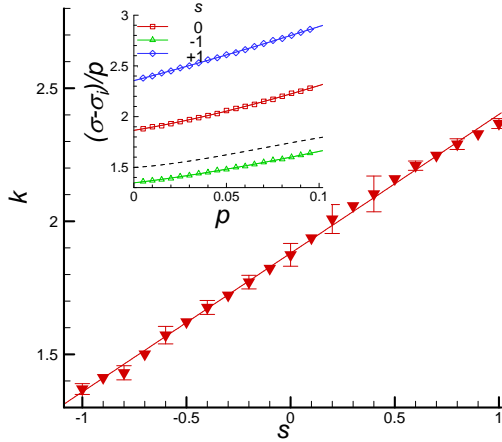


Fig. 9. Intrinsic conductivity k vs. parameter s . In the inset: $(\sigma/\sigma_i - 1)/p$ vs. p for $s = 0, \pm 1$ (symbols) and for conventional random site percolation (dash line). The data correspond to $L \rightarrow \infty$. [36].

However, the situation changes drastically if occupation probability is rather small $p < 0.1$. At given p , increase of s leads to decrease of σ . The conductivity is maximum when all the dimers are aligned along the conductivity direction (see left inset in Fig. 7). If p is small enough, the conductivity behaviour can be well fitted by virial expansion [37]

$$\sigma/\sigma_i = 1 + kp + mp^2 + \dots, \quad (12)$$

where k and m are the adjustable parameters.

The value of intrinsic conductivity k can be extracted from $(\sigma/\sigma_i - 1)/p$ vs. p in the limit of $p \rightarrow 0$ (see inset in Fig. 9).

Intrinsic conductivity k as a function of orientation order parameter s is fitted well by linear function $k = 1.88 + 0.52s$ (with correlation $\rho = 0.9976$) (Fig. 9). Notice that intrinsic conductivity calculated for conventional random site percolation (percolation of monomers) is 1.50 ± 0.01 (dash line in inset in Fig. 9).

4 Conclusion

Thus, new percolation problem, i.e. percolation of aligned dimers on a square lattice, was proposed and studied. The percolation threshold for deposition of dimers was lower than for deposition of monomer, $p_c = 0.5927\dots$, nevertheless, the problem belongs to the same universality class.

The lowest percolation threshold $p_c = 0.562$ corresponds to isotropic orientation of the dimers ($s = 0$). In the case of dimers aligned strictly along one direction ($s = +1, -1$), the percolation point is $p_c = 0.586$. Near the point of percolation transition ($p \rightarrow p_c$), the conductivity essentially decreases if the absolute value of orientation order parameter $|s|$ increases. Intrinsic conductivity k increases linearly with s ($k = 1.88 + 0.52s$) and differs from the known value for a lattice filled with monomers $k = 1.50 \pm 0.01$.

The proposed model can be applied to the phase transitions of anisotropic objects on a lattice when their concentration and orientation are varied. In particular, the model is useful for description of a phase transition from insulator to (semi)conductor upon aligned deposition of the prolate objects on a substrate. The natural extension of the model is substitution of dimers by k -mers and inclusion of the bonds between the dimers into consideration.

5 Acknowledgment

This work has been supported by Russian Foundation for Basic Research (grant no. 09-02-90440) and Ministry of Education and Science of Ukraine (Project no F28.2/058).

References

1. G. Grimmet, *Percolation* (Berlin: Springer-Verlag, 1999)
2. H. Kesten, *Percolation theory for mathematicians* (Boston: Birkhauser, 1982)
3. J. Feder, *Fractals* (New York: Plenum Press, 1988)
4. J.M. Ziman, *Models of disorder. The Theoretical Physics of Homogeneously Disordered Systems* (Cambridge University Press, 1979)
5. B.I. Shklovskii, A.L. Efros, *Electronic properties of doped semiconductors* (Springer, Heidelberg, 1984)
6. D. Stauffer, A. Aharony, *Introduction to Percolation Theory* (Taylor & Francis, 1992)
7. I. Sahimi, *Application of Percolation Theory* (London: Taylor & Francis, 1994)
8. F. Du, J.E. Fischer, K.I. Winey, *Phys. Rev. B* **72**, 121404 (2005)
9. D. L. Carroll, R. Czerw, S. Webster, *Synthetic Metals* **155**, 694 (2005)
10. T.V. Sree Kumar, T. Liu, S. Kumar, L.M. Ericson, R.H. Hauge, R.E. Smalley, *Chem. Mater* **15**, 175 (2003)
11. Y. Zhou, A. Gaur, S-H. Hur, C. Kocabas, M.A. Meitl, M. Shim, J.A. Rogers, *Nano Letters* **4**, 1643 (2004)
12. A.Yu. Dovzhenko, V.A. Bunin, *Technical Physics* **48**, 123 (2003)
13. G. Kondrat, A. Pękalski, *Phys. Rev. E* **63**, 051108 (2001)
14. N.V. Vygornitskii, L.N. Lisetskii, N.I. Lebovka, *Colloid Journal* **69**, 597 (2007)
15. X. Liu, J.L. Spencer, A.B. Kaiser, W.M. Arnold, *Current Applied Phys.* **4**, 125 (2004)
16. C. Park, J. Wilkinson, S. Banda, Z. Ounaies, K.E. Wise, G. Sauti, P. T. Lillehei, J.S. Harrison, *Journal of Polymer Science Part B: Polymer Physics* **44**, 1751 (2006).
17. J.W. Evans, *Rev. Mod. Phys* **65**, 1281 (2003)
18. Z. Adamczyk, *Particles at Interfaces: Interactions, Deposition, Structure* (Academic Press, 2006)
19. H. Holloway, *Phys. Rev. B* **37**, 874 (1988)
20. J.W. Evans, D.E. Sanders, *Phys. Rev. B* **39**, 1587 (1989)
21. Y. Leroyer, E. Pommiers, *Phys. Rev. B* **50**, 2795 (1994)
22. N. Vandewalle, S. Galam, M. Kramer, *Eur. Phys. J. B* **14**, 407 (2000)
23. J. Cortes, E. Valencia, *J. Colloid & Interface Sci.* **252**, 256 (2002)
24. V. Cornette, A. J. Ramirez-Pastor, F. Nieto, *Physica A* **327**, 71 (2003)

25. V. Cornette, A. J. Ramirez-Pastor, F. Nieto, Eur. Phys. J. B **36**, 391 (2003)
26. V. Cornette, A. J. Ramirez-Pastor, F. Nieto, Physics Letters A **353**, 452 (2006)
27. M. Quintana, I. Kornhauser, R. Lopez, A.J. Ramirez-Pastor, G. Zgrablich, Physica A **361** 195 (2006).
28. M. Dolz, F. Nieto, A.J. Ramirez-Pastor, Physica A **374** 239 (2007)
29. G. Pruessner, M. Moloney, J. Phys. A **36**, 11213 (2003)
30. M. Matsumoto, ACM Trans. on Modeling and Computer Simulations **8**, 3 (1998)
31. D.A. Matoz-Fernandez, D.H. Linares, A.J. Ramirez-Pastor, EPL **82**, 50007 (2008)
32. J. Hoshen, R. Kopelman, Phys. Rev. B **14**, 3438 (1976)
33. D.J. Frank , C.J. Lobb, Phys. Rev. B **37**, 302 (1988)
34. Y. Yuge , K. Onizuka, J. Phys. C: Solid State Phys. **11**, 4095 (1978)
35. A. Bunde, S. Havlin, *Fractals and Disordered Systems*, eds. A. Bunde and S. Havlin (Springer, 1996)
36. C.J. Lobb , D.J. Frank, Phys. Rev. B **30**, 4090 (1984)
37. E.J. Garboczi , K.A. Snyder, J.F. Douglas, Phys. Rev. E **52**, 819 (1995)